J Mol Model (2010) 16:1195–1204
DOI 10.1007/s00894-009-0630-y

ORIGINAL PAPER

Structure-based and shape-complemented pharmacophore modeling for the discovery of novel checkpoint kinase 1 inhibitors

Xiu-Mei Chen · Tao Lu · Shuai Lu · Hui-Fang Li · Hao-Liang Yuan · Ting Ran · Hai-Chun Liu · Ya-Dong Chen

Received: 27 August 2009 / Accepted: 18 November 2009 / Published online: 18 December 2009
© Springer-Verlag 2009

Abstract Checkpoint kinase 1 (Chk1), a member of the serine/threonine kinase family, is an attractive therapeutic target for anticancer combination therapy. A structure-based modeling approach complemented with shape components was pursued to develop a reliable pharmacophore model for ATP-competitive Chk1 inhibitors. Common chemical features of the pharmacophore model were derived by clustering multiple structure-based pharmacophore features from different Chk1-ligand complexes in comparable binding modes. The final model consisted of one hydrogen bond acceptor (HBA), one hydrogen bond donor (HBD), two hydrophobic (HY) features, several excluded volumes and shape constraints. In the validation study, this feature-shape query yielded an enrichment factor of 9.196 and performed fairly well at distinguishing active from inactive compounds, suggesting that the pharmacophore model can serve as a reliable tool for virtual screening to facilitate the discovery of novel Chk1 inhibitors. Besides, these pharmacophore features were assumed to be essential for Chk1 inhibitors, which might be useful for the identification of potential Chk1 inhibitors.

Keywords Checkpoint kinase 1 · Inhibitor · Shape · Structure-based pharmacophore

X.-M. Chen · T. Lu · S. Lu · H.-F. Li · H.-L. Yuan · T. Ran · H.-C. Liu · Y.-D. Chen (✉)
Laboratory of molecular design and drug discovery,
China Pharmaceutical University,
24 Tongjiaxiang,
Nanjing 210009, People's Republic of China
e-mail: ydchen@cpu.edu.cn

Introduction

Checkpoint kinase 1(Chk1), a serine/threonine kinase, is a key regulator of cell cycle progression and DNA repair [1], which has emerged as a novel target for anticancer combination therapy [2]. Inhibition of Chk1 has been shown to abrogate cell cycle arrest to sensitize the efficacy of DNA-damaging agents or radiation, leading to enhanced tumor cell death [3, 4]. The discovery of novel Chk1 inhibitors is an intensely studied field [5–7], and the most advanced agents are now in the early phase of clinical development [8], such as UCN-01, PF-00477736, and AZD7762 (see Fig. 1). Among them, PF-00477736 is a potent, selective ATP-competitive small-molecule Chk1 inhibitor [4].

The ATP binding pocket of Chk1 can be roughly divided into five regions [9, 10]: the solvent-exposed region, the hinge region, the water pocket, the polar region, and the ribose binding pocket (see Fig. 2). The solvent-exposed region is adjacent to the hinge region, and the introduction of the polar group pointing to the solvent-accessible region might gain desirable enzymatic potency and prove amenable for the modulation of biophysical characteristics [11–13]. The water pocket, which is unique to Chk1, is occupied by three water molecules and buried at the periphery of the ATP binding site. It has been demonstrated that filling this pocket can confer ligands with enhanced affinity for Chk1 [9, 14]. In addition, to obtain high potency, it is required for the ligands to form hydrogen bond interactions with amino acid residues in the polar region [15]. Another characteristic is the tendency of ligands to form ionic interactions with the acidic residue (Glu91) or hydrogen bond interactions with the side chain carbonyl oxygen of Glu91, situated at the ribose binding

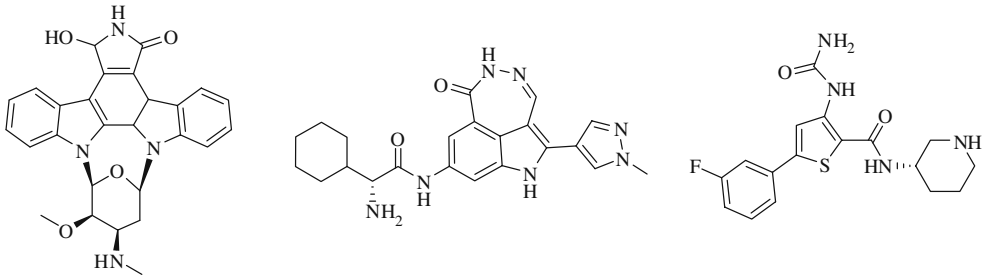

Fig. 1 Structures of selected published clinical candidate Chk1 inhibitors

pocket [16–18]. It has been revealed that this region is of great significance [19], for functional groups designed to interact with residues in or in proximity to the ribose binding pocket were desired despite not a specific requirement for inhibition of Chk1. Details on the hinge region are discussed in the section below. It remains unclear that which regions are essential for the rational design of inhibitors targeting Chk1, so it is necessary to gain further insight into the structural requirements of Chk1 inhibitors.

Pharmacophore modeling is one of the most successfully used tools in drug discovery and design [20, 21], which provides useful information to understand the interactions between a target protein and a ligand. The pharmacophore model is a set of chemical features aligned in three-dimensional (3D) space. This spatial arrangement of chemical features represents the essential interactions between ligands and proteins [22].

The traditional pharmacophore modeling, based on a series of available ligands, has been the primary thrust in virtual screening for a long time. In the absence of structural data of the target protein, ligand-based pharmacophore has been a considerably successful tool for virtual screening technology. The ligand-based pharmacophore model of Chk1 inhibitors has been reported by Chen et al. [23], which was derived from a set of structurally diverse Chk1 inhibitors without explicit knowledge of the receptor structure. However, with the rapidly growing number of crystal structures of Chk1-ligand complexes resolved, it is possible to develop the structure-based pharmacophore model [24, 25]. Since the structure-based pharmacophore model maintains an adequate geometric relationship of the active sites and is less dependent on the known Chk1 inhibitors compared with ligand-based pharmacophore model, it is expected that it will improve the novelty of the hit list once used for the virtual screening.

In this study, we have focused on the generation of pharmacophore models of ATP-competitive Chk1 inhibitors from available 3D crystal complexes, complemented with shape component of the inhibitors. The structure-based pharmacophore model is able to present the intermolecular interactions between Chk1 and its ligands in a visual and straightforward way. Moreover, to obtain good shape complementarity for the ligands with the ATP binding pocket of Chk1, shape components were utilized to optimize the pharmacophore models. Once the pharmacophore model is identified, it can be used as a powerful tool for the discovery and development of new hit compounds. Currently, a total of 35 crystal structures of Chk1-ligand

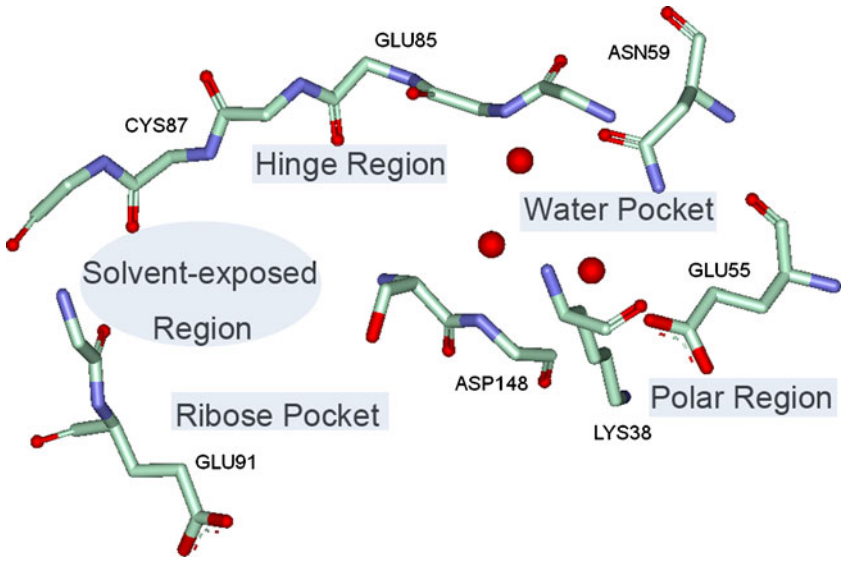

Fig. 2 Five specific regions of the ATP binding pocket of Chk1

complexes are available in the Protein Data Bank (PDB) [26]. The pharmacophore features were detected by software LigandScout [24] based on these crystal structures. Common chemical features were attained by clustering multiple structure-based pharmacophore features among different bound ligands of Chk1 complexes. Excluded volume spheres and shape constraints were also included in the model to further improve selectivity. Then the resultant pharmacophore models were validated by screening a validation database spiked with known Chk1 inhibitors. It is hoped that the present study can provide valuable information of pharmacophoric interactions between Chk1 and different inhibitors, and facilitate the discovery of promising Chk1 inhibitors.

Materials and methods

Generation of structure-based pharmacophore models

A set of 35 crystal structures of Chk1 in complex with diverse ligands were obtained from the Protein Data Bank (PDB) (see Fig. 3). Water molecules have been reported to play a crucial role in mediating the interactions between ligands and Chk1 [9], and those in ligand-binding sites can provide useful information for the process of pharmacophore construction [27]. Therefore, all the water molecules in the crystal structures were retained. The coordinates of 35 Chk1-ligand X-ray crystal structures were transformed into a common reference frame using multiple structure alignment within Accelrys Discovery Studio 2.1 [28].

Individual pharmacophore models were generate based on the previously aligned structures using the software LigandScout 2.02 [24], which uses an algorithm that allows the automatic construction of the pharmacophore model from the structural data of the protein-ligand complex. Moreover, excluded volumes were also automatically included in the models by the software [29]. Next, the pharmacophore models were imported as hypotheses into Catalyst by the hypoedit tool from LigandScout [30]. As two chemical features cannot be placed onto one structural element in Catalyst [31], several complementary pharmacophore models were generated to describe the binding site. Then all of the pharmacophore features except excluded volumes in the pharmacophore models were clustered according to interaction patterns of ligands with Chk1. The hydrophobic features were clustered with an interactive dendrogram for the selection of cluster centers. Three cluster centers of the hydrogen bond acceptor features in the hinge region, the water pocket (corresponding to three water molecules) and the polar region were identified after hierarchical clustering within the Accelrys Discovery Studio [28]. The cluster centers of the hydrogen bond donor features were identified in the same way. Subsequently, the constructed model was refined by the modification of the constraint tolerance of the spheres in accordance with the default values of Catalyst software [30]. Additionally, excluded volume spheres were used as steric constraints. Finally, the pharmacophore was complemented with shape constraints to account for the shape complementarity of ligands with the ATP binding pocket of Chk1.

Validation of the pharmacophore model *via* retrospective discovery of known Chk1 inhibitors

One of the standard approaches to validate computational models is to perform the retrospective analysis. Herein, we constructed a validation database consisting of 60 known Chk1 inhibitors and 1291 randomly sampled compounds. The randomly sampled set served as decoys, which were obtained from a collection offered by drugbank [32] (subset of random FDA-approved small molecule drug structures without biological activities on Chk1 reported). The known Chk1 inhibitors consisted of seven drug candidates in preclinical or clinical development [7–9] and 53 compounds collected from several literatures published by Abbott Laboratories [10, 11, 13, 33–35]. It is worth noting that three drug candidates in clinical development (UCN-01, PF-00477736, and AZD7762) were in the validation database. In addition, the biological activity data of the 53 compounds was measured by similar Chk1 enzymatic assay procedures (39 active compounds on Chk1, $IC_{50}<100$ nM; 14 inactive compounds, $IC_{50}>10000$ nM). Thus a total of 1351 compounds were successfully converted into a searchable multiconformer database by using the catDB command (FAST method, maximum number of conformers=100). Then all screening experiments were performed by using the Fast Flexible Search algorithm in Catalyst [36].

Results and discussion

Structure-based pharmacophore models

A prerequisite for the generation of the structure-based model is the knowledge on the target-ligand interactions including the availability of the 3D structure of the target by X-ray crystallography, NMR or protein homology modeling studies. And a crystal complex with a ligand bound to the active site of the protein is required for the construction of the structure-based pharmacophore model. Generally, the structure-based pharmacophore model is generated based on an individual crystal complex, which might not be so reliable just reflecting a single interaction pattern. Thus, in the case of a set of Chk1 crystal complexes available, there

is a great chance to cover sufficient interaction patterns and detect common pharmacophore features for an acceptable pharmacophore model.

To find common chemical features from different bound Chk1 inhibitors with comparable binding modes, cluster analysis was implemented for multiple pharmacophore features. In total, there were 47 pharmacophore models constructed by LigandScout based on the 35 aligned crystal structures of Chk1 (see Fig. 4). Most of the inhibitors showed favorable hydrophobic contacts with hydrophobic cleft of the Chk1. As a result, two cluster centers of hydrophobic features constituted a major part of the pharmacophore models, in agreement with the overall hydrophobic nature of the active site of Chk1. One was surrounded by hydrophobic residues Val23 and Tyr20, the other by residues Leu15 and Leu137. The positive ionizable features located in the ribose binding pocket were not included in our pharmacophore models since they were not specific requirement for the inhibition of Chk1 as mentioned above. The hydrogen bond features detected were mainly located in the hinge region, the water pocket and the polar region. Those frequently detected ones are listed in Table 1. According to frequency of occurrence in different regions, three acceptor cluster centers were selected, corresponding to Cys87 in the hinge region (HR-Acceptor), three water molecules in the water pocket (WP-Acceptor), and Lys38 in the polar region (PR-Acceptor). Likewise, the donor cluster center was chosen, mapping onto Glu85 in the hinge region (HR-Donor). Then it was of great importance to determine which hydrogen bond features should be involved in the pharmacophore model.

Previous study indicated that the interaction with the hinge region is essential for potent Chk1 inhibition [9], which is consistent with the high statistical frequency of the features detected in the hinge region. There are different hinge binding patterns observed in the crystal structures of Chk1-ligand complexes [10]. One of the commonly found patterns is the formation of hydrogen bonds between the ligands with the backbone NH of Cys87 and the backbone carbonyl of Glu85 (see Fig. 4), summing up to one acceptor cluster center (HR-Acceptor) and one donor cluster center (HR-Donor) in our initial pharmacophore model (see Fig. 5a, Hypo1). We kept these features (two hydrophobic features, HR-Acceptor, HR-Donor) as a starting point, and the features in other regions would be evaluated in the section below. The ligand-based pharmacophore model generated by Chen et al. [23] showed the hydrogen bond interaction between the inhibitors and the amino acid residues in the hinge region (Cys87, Glu85), which also substantiated the model Hypo1.

To further improve selectivity, the initial model Hypo1 was optimized by adding so-called excluded volume spheres [37], which resembled sterically inaccessible regions within the binding site. Twelve excluded volume features were found in the ATP-binding site, whose spaces were occupied by residues Leu15, Gly16, Tyr20, Val23, Tyr86, Cys87, Glu90, Glu134, Asn135, Leu137, and Asp148. These excluded volume features were automatically detected by LigandScout based on one representative aligned crystal structure. The resultant pharmacophore model Hypo2 with excluded volume spheres is shown in Fig. 5b.

It is suggested that ConFirm module within Catalyst is able to generate the low-energy conformations similar to those present in the protein-ligand complexes [38]. Moreover, one may wonder whether Hypo2 can capture the mapping conformation close to the bioactive conformation. When mapped onto Hypo2 by choosing “Fast Fit” option, the bound conformation of the macrocyclic urea compound from the crystal complex (PDB entry: 2E9U) fit quite well with all the features of the pharmacophore. Meanwhile, the Catalyst conformations generated by ConFirm module were mapped onto Hypo2 with the same option to verify whether the method could find the correct bioactive conformation (see Fig. 5c). The root mean square distance (RMSD) between the heavy atom positions of the bound and the mapping Catalyst conformation was 1.05 Å. Hence, Hypo2 may be utilized to determine the bioactive conformations of the ligands that share the same binding mode.

Subsequently, the pharmacophore Hypo2 was complemented with shape constraints based on the shape of the drug candidates having entered clinical trials. It is not clear yet whether different selectivity profiles against Chk1 and Chk2 (checkpoint kinase 2) could lead to different clinical outcomes. Whereas UCN-01 and AZD7762 are approximately equipotent against Chk1 and Chk2, PF-00477736 is almost 100-fold selective for Chk1 over Chk2 [7, 39]. Moreover, PF-00477736 has the appropriate chemical features for binding and has the proper shape to fit into the ATP binding pocket of Chk1. Thus PF-00477736 was chosen to generate a shape component based on the low energetic conformers *via* the algorithm CatShape within Catalyst [40]. In order to create a feature-shape query (containing both hypothesis and shape), “Fast Fit” option was used to map Hypo2 onto the low energetic conformers of PF-00477736. With the mapping displayed, the conformer was converted into a shape query, and then the hypothesis query with a merged shape was built in an appropriate alignment (see Fig. 5d, Hypo3). The shape constraints were relaxed by changing the Minimum Similarity Tolerance to 0.41 (the default is 0.50), making the query less restrictive [30]. All other parameters used were kept as default.

Fig. 3 Ligand structures from 35 Chk1 protein-ligand complexes ▶ used in this study

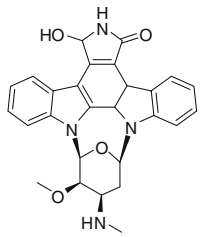
1NVQ

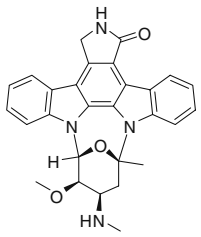
1NVR

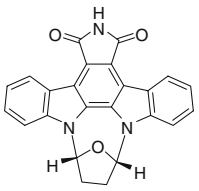
1NVS

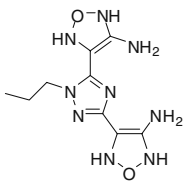
2CGW

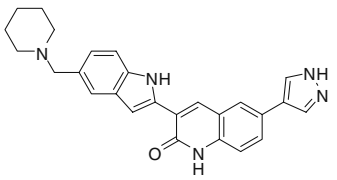
2HY0

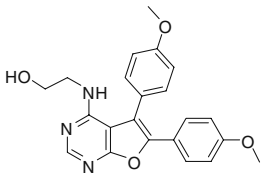
2BR1

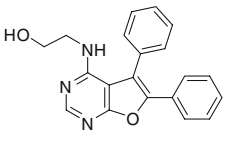
2BRB

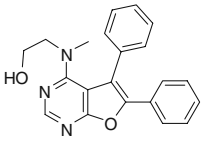
2BRG

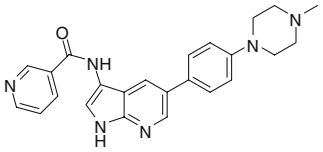
1ZYS

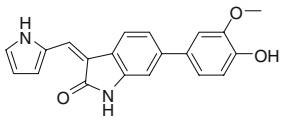
2AYP

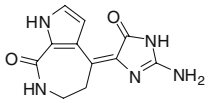
2C3J

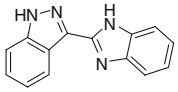
2C3L

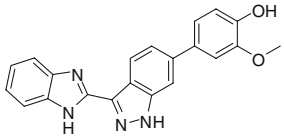
2C3K

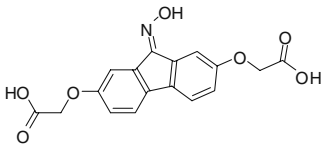
2CGU

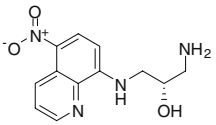
2CGV

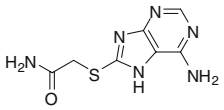
2CGX

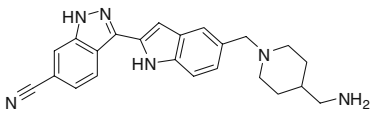
2HXL

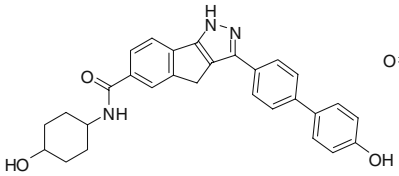
2E9N

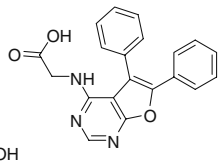
2BRH

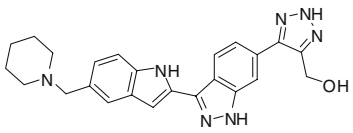
2HOG

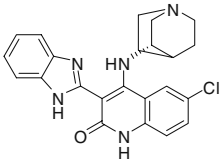
2GDO

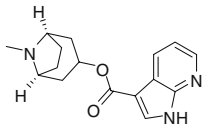
2QHM

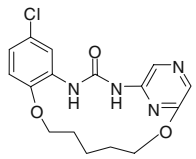
2E9U

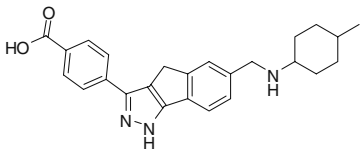
2E9O

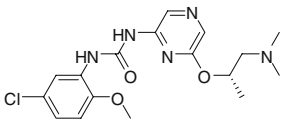
2E9P

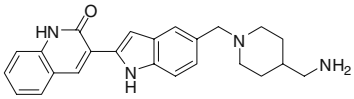
2HXQ

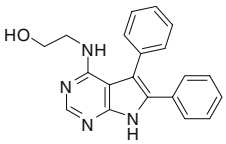
2BRM

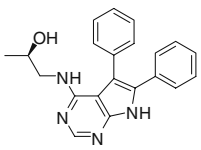
2BRN

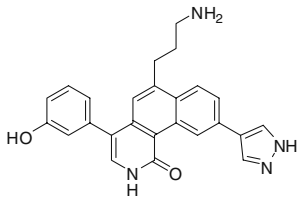
2R0U

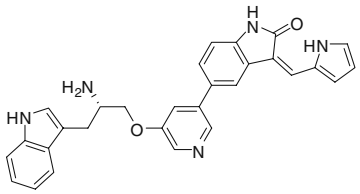
2GHG

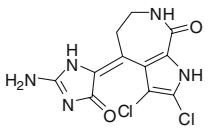
1ZLT

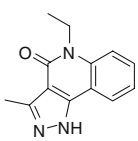
2QHN

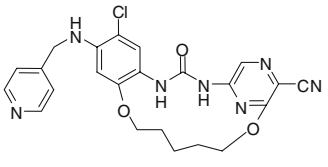
2E9V

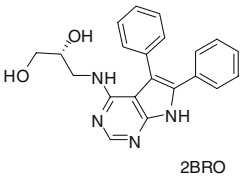
2BRO

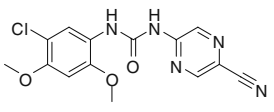
2YWP

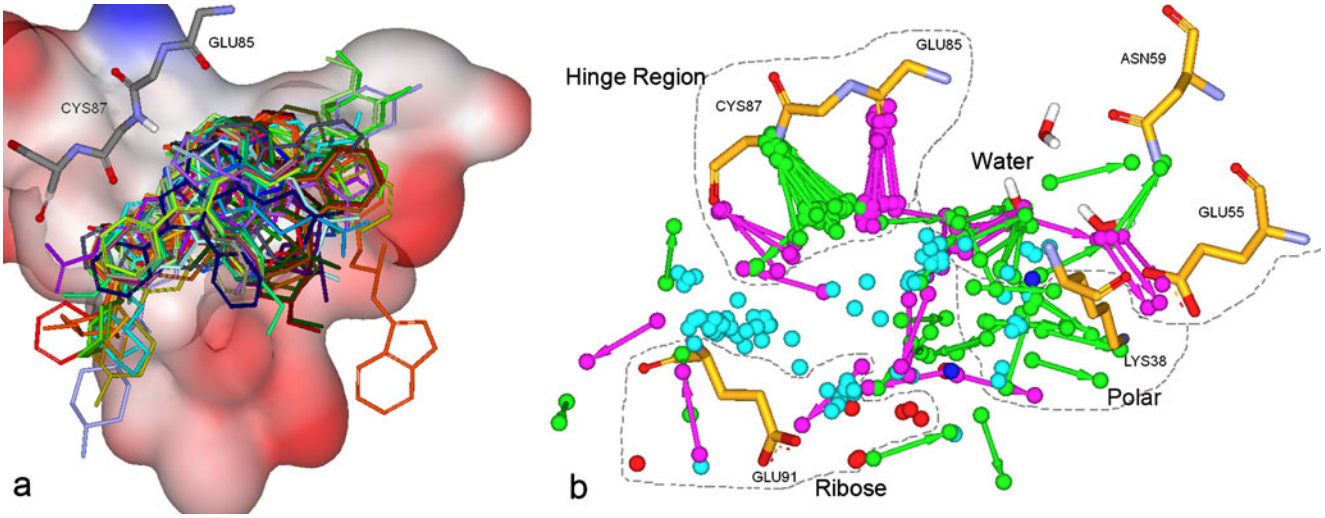

Fig. 4 (**a**) Multiple structure alignment according to their 3D structural similarity and the ligands are in a common reference frame. Coloring surface of one representative aligned protein structure using electrostatic potential. Every ligand is in a different color. (**b**) The pharmacophore features generated using LigandScout based on the previously aligned protein structures. Features of the pharmacophore models are color-coded as follows: hydrogen bond acceptor (HBA), green; hydrogen bond donor (HBD), violet; hydrophobic (HY), light blue; positive ionizable, red; negative ionizable, blue

Validation of the pharmacophore model *via* retrospective discovery of known Chk1 inhibitors

For the hits retrieved by the initial pharmacophore model Hypo1, there were 44 active compounds, 14 inactive compounds, 589 decoys. More careful inspection of the hit list indicated that many of the false positives (hits retrieved from inactive compounds and decoys) possessed bulky, or unusually long side chains, which were actually far too large to fit into the ATP binding pocket of Chk1.

However, after excluded volume spheres and shape constraints were added to the initial model Hypo1, the results were significant since the feature-shape pharmacophore Hypo3 could effectively prune and focus the hit list. In detail, 99 hits were retrieved by the refined pharmacophore model Hypo3 from the validation database, consisting of 31 active compounds and 68 false positives (one inactive compound and 67 decoys). As mentioned above, the validation database contained 1351 molecules, in which 46 were active Chk1 inhibitors. Thus, the enrichment factor (E, see Eq. 1) calculated according to Ananthula et al. [41] was 9.196, indicating that it was 9.196 times more probable to pick an active compound from the database than an inactive one. Notably, two inhibitors in the clinical phase (PF-00477736 and AZD7762) were retrieved except UCN-01, which showed the selectivity of generated hypothesis to some extent.

$$E = \frac{Ha/Ht}{A/D} \quad (1)$$

where Ht=the number of hits retrieved, Ha=the number of actives in the hit list, A=the number of active molecules present in the database, and D=the total number of molecules in the database.

The receiver operating characteristic (ROC) curve was also used to estimate the performance of the feature-shape pharmacophore model Hypo3 [42]. It can be used to help understand the tradeoff between model sensitivity (ability

Table 1 Hydrogen bond features detected by LigandScout[a]

Features	Count	Interaction	Find cluster center
Acceptor	42	HR: the backbone NH of Cys87	Yes: HR-Acceptor
Donor	20	HR: the backbone carbonyl oxygen of Glu85	Yes: HR-Donor
Acceptor	12	WP: three water molecules	Yes: WP-Acceptor
Donor	8	HR: the backbone carbonyl oxygen of Cys87	No
Acceptor	6	PR: the side chain NH of Lys38	Yes: PR-Acceptor
Donor	6	WP: three water molecules	No
Acceptor	3	WP: the side chain NH of Asn59	No
Donor	3	WP: the side chain carbonyl oxygen of Glu55	No
Donor	1	RP: the side chain carbonyl oxygen of Glu91	No

[a] Hydrogen bond features interacting with waters not in the water pocket have not been listed in this Table for clarity. HR, the hinge region; PR, the polar region; WP, the water pocket; RP, the ribose binding pocket

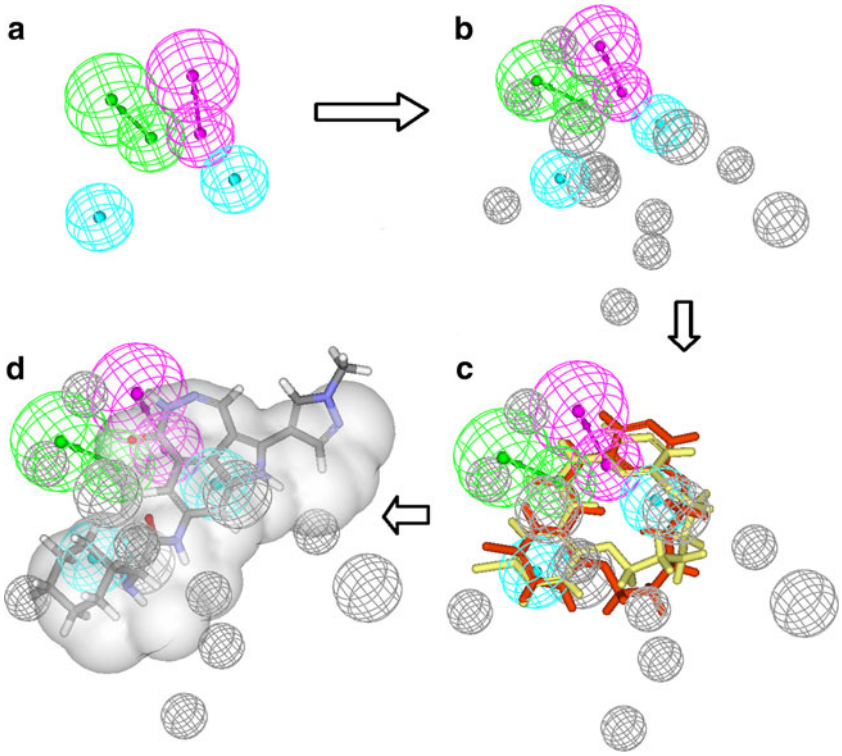

Fig. 5 Flowchart of the generation of the structure-based pharmacophore model. (**a**) The initial hypothesis model (Hypo1). (**b**) The refined pharmacophore model augmented with excluded volumes (Hypo2). (**c**) Bioactive conformation determination. The mapping Catalyst conformation of the macrocyclic urea compound (red stick model) and the bound conformation (yellow stick model) from the crystal structure are superimposed on Hypo2. (**d**) The feature-shape query (Hypo3) obtained by superimposition and merging of PF-00477736 shape and Hypo2. Screenshots were taken from Discovery Studio. Features of the pharmacophore models are color-coded as follows: hydrogen bond acceptor (HBA), green; hydrogen bond donor (HBD), violet; hydrophobic (HY), light blue. The Catalyst shape is displayed as a gray cloud

to discover true positives) and specificity (ability to avoid false positives). The fit property of the compounds, which indicates the degree of consistency with the model Hypo3, was calculated in Catalyst. Thus, the fit values were used to rank the 1351 compounds in the validation database according to their predicted likelihood of being "good" or "bad". The ROC score (the area under the ROC curve, AUC) provides a practical way of measuring the overall performance of the model. The closer the ROC score is to 1.0, the better the model is at distinguishing good samples from bad ones. ROC curve analysis of the model Hypo3 yielded the ROC score of 0.817 (see Fig. 6), which means that in eight out of ten cases, a randomly selected active Chk1 inhibitor is ranked higher than an inactive one. This validation has given additional confidence in the utility of the selected pharmacophore model.

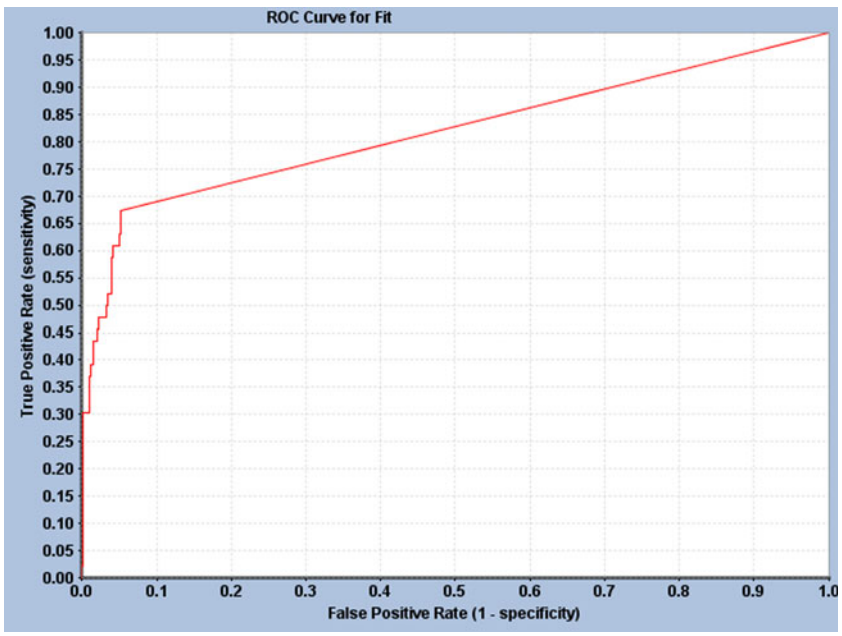

Fig. 6 The performance of the feature-shape pharmacophore model Hypo3 analyzed using ROC curves. The long straight line up to the top right hand corner of the ROC curve revealed that some of the actives scored no more than decoys. It was generated using component "ROC Plot Viewer" in the Pipeline Pilot [43]

Table 2 Statistical Parameters from Screening of validation database

	Parameter	Hypo3	Hypo4(Polar)	Hypo5(Water)
1	total molecules in database (D)		1351	
2	total no. of actives in database (A)		46	
3	total hits (Ht)	99	55	27
4	active hits (Ha)	31	24	8
5	enrichment factor (E)	9.196	12.815	8.702
6	ROC score for Fit[a]	0.817	0.750	0.503

[a] ROC Score: The area under the curve of the ROC plot derived from the data

Evaluation of the cluster centers of hydrogen bond features in other regions

To explore whether aforementioned PR-Acceptor in the polar region should be merged in the pharmacophore model, two pharmacophore models Hypo4 and Hypo5 were constructed by combining Hypo3 with the PR-Acceptor feature in polar region and WP-Acceptor in the water pocket, respectively. These pharmacophore models were then used to retrospectively screen known Chk1 inhibitors, and the screening results were shown in Table 2. Although Hypo4 achieved the best enrichment factor, it failed to outweigh Hypo3 in the ROC analysis. Moreover, Hypo3 picked out the maximum number of active inhibitors even though it could not reject maximum number of false positives. Presumably, additional hydrogen bond features in the polar region or the water pocket are not essential for Chk1 inhibition but they might be beneficial for ligand potency.

Comparison of structure-based pharmacophore with ATP binding pocket of Chk1

To further evaluate Hypo3, the feature-shape pharmacophore model was mapped into the ATP binding pocket of Chk1 (see Fig. 7). Non-covalent interactions and shape complementarity are believed to prompt protein-ligand interactions. The hydrogen bond features displayed the hydrogen bond interactions between ligands and the conserved kinase backbone binding motif in the hinge region. The hydrophobic features exhibited extensive hydrophobic contacts with the backbone and/or side chains of residues, such as Leu15, Tyr20, Val23, and Leu137. The excluded volume features corresponded to the positions that were inaccessible for any potential ligands. The shape components filled the ATP-binding site quite well. In conclusion, the chemical features and their spatial arrangement described in the feature-shape pharmacophore model Hypo3 were consistent with the essential protein-ligand interactions.

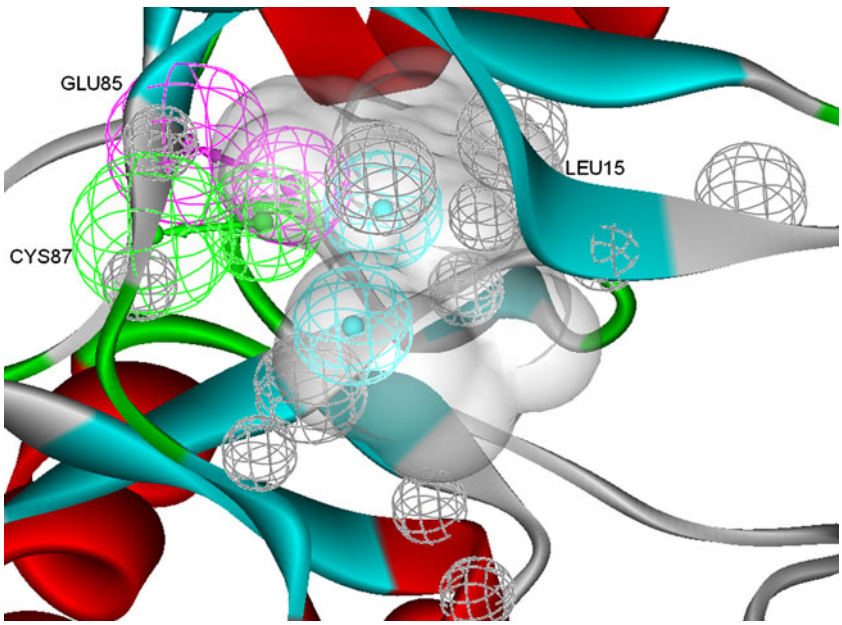

Fig. 7 The mapping of feature-shape Hypo3 with the ATP binding pocket of Chk1. Glu85 and Cys87 are part of the conserved kinase backbone binding motif in the hinge region. Screenshots were taken from Discovery Studio. Features of the pharmacophore models are color-coded as follows: hydrogen bond acceptor (HBA), green; hydrogen bond donor (HBD), violet; hydrophobic (HY), light blue. The Catalyst shape is displayed as a gray cloud

Chen et al. [23] have also made the comparison analysis of the aforementioned ligand-based pharmacophore model with chemical features in the ATP binding pocket of Chk1. The hydrogen bond features of the ligand-based pharmacophore model corresponded to HR-Acceptor and HR-Donor in the model Hypo3, which reflected the interactions between ligands and the hinge region. Besides, two hydrophobic features existed in both models. However, the 12 excluded volume features in the model Hypo3, were different from only one excluded volume in the ligand-based model based on the known Chk1 inhibitors. In light of the structural data of the protein-ligand complexes, the excluded volume features in the model Hypo3 may be of advantage to characterize the steric limitations of the binding site.

Conclusions

Mounting evidence has indicated that Chk1 inhibitors have potential therapeutic application in sensitizing DNA-damaging agents or radiation to combat cancers. In the present study, we took advantage of the information from the Protein Data Bank (PDB) to develop pharmacophore models of the ATP-competitive Chk1 inhibitors. Common chemical features were obtained by clustering multiple structure-based pharmacophore features. Excluded volume spheres and shape constraints based on the low energetic conformers of PF-00477736 were also included in the model to further improve selectivity. The final feature-shape model Hypo3 consisted of spatial arrangement of chemical features: one hydrogen bond acceptor (HBA), one hydrogen bond donor (HBD), two hydrophobic (HY) features, several excluded volumes and shape constraints. These hydrogen bond features were mainly located in the hinge region. Nevertheless, it is worth noting that features in other binding regions (such as the polar region and the water pocket) may also be involved in the rational combinations of pharmacophore features. However, the validation study showed that Hypo3 gave an enrichment factor of 9.196 and performed better at distinguishing active from inactive compounds in the validation database. It is expected that the information provided here is helpful for the study toward more reliable pharmacophore modeling of Chk1 inhibitors, which can be used for virtual screening to discover novel potential hit compounds.

Acknowledgments The authors gratefully acknowledge the Inte: Ligand GmbH for providing the academic license of the LigandScout 2.02. This work was supported by Qing Lan Project of Jiangsu province in China.

References

1. Ashwell S, Janetka JW, Zabludoff S (2008) Keeping checkpoint kinases in line: new selective inhibitors in clinical trials. Expert Opin Investig Drugs 17:1331–1340. doi:10.1158/1078-0432.CCR-07-5138
2. Tse AN, Carvajal R, Schwartz GK (2007) Targeting checkpoint kinase 1 in cancer therapeutics. Clin Cancer Res 13:1955–1960. doi:10.1158/1078-0432.CCR-06-2793
3. Tse AN, Rendahl KG, Sheikh T, Cheema H, Aardalen K, Embry M, Ma S, Moler EJ, Ni ZJ, Lopes de Menezes DE, Hibner B, Gesner TG, Schwartz GK (2007) CHIR-124, a novel potent inhibitor of Chk1, potentiates the cytotoxicity of topoisomerase I poisons in vitro and in vivo. Clin Cancer Res 13:591–602. doi:10.1158/1078-0432.CCR-06-1424
4. Blasina A, Hallin J, Chen E, Arango ME, Kraynov E, Register J, Grant S, Ninkovic S, Chen P, Nichols T, O'Connor P, Anderes K (2008) Breaching the DNA damage checkpoint via PF-00477736, a novel small-molecule inhibitor of checkpoint kinase 1. Mol Cancer Ther 7:2394–2404. doi:10.1158/1535-7163.MCT-07-2391
5. Prudhomme M (2006) Novel checkpoint 1 inhibitors. Recent Patents Anticancer Drug Discov 1:55–68
6. Arrington KL, Dudkin VY (2007) Novel inhibitors of checkpoint kinase 1. ChemMedChem 2:1571–1585. doi:10.1002/cmdc.200700131
7. Janetka JW, Ashwell S, Zabludoff S, Lyne P (2007) Inhibitors of checkpoint kinases: from discovery to the clinic. Curr Opin Drug Discov Dev 10:473–486
8. Ashwell S, Zabludoff S (2008) DNA damage detection and repair pathways-recent advances with inhibitors of checkpoint kinases in cancer therapy. Clin Cancer Res 14:4032–4037. doi:10.1158/1078-0432.CCR-07-5138
9. Tao ZF, Lin NH (2006) Chk1 inhibitors for novel cancer treatment. Anticancer Agents Med Chem 6:377–388
10. Wang L, Sullivan GM, Hexamer LA, Hasvold LA, Thalji R, Przytulinska M, Tao ZF, Li G, Chen Z, Xiao Z, Gu WZ, Xue J, Bui MH, Merta P, Kovar P, Bouska JJ, Zhang H, Park C, Stewart KD, Sham HL, Sowin TJ, Rosenberg SH, Lin NH (2007) Design, synthesis, and biological activity of 5, 10-dihydro-dibenzo[b, e][1, 4]diazepin-11-one-based potent and selective Chk-1 inhibitors. J Med Chem 50:4162–4176. doi:10.1021/jm070105d
11. Hasvold LA, Wang L, Przytulinska M, Xiao Z, Chen Z, Gu WZ, Merta PJ, Xue J, Kovar P, Zhang H, Park C, Sowin TJ, Rosenberg SH, Lin NH (2008) Investigation of novel 7, 8-disubstituted-5, 10-dihydro-dibenzo[b, e][1, 4]diazepin-11-ones as potent Chk1 inhibitors. Bioorg Med Chem Lett 18:2311–2315. doi:10.1016/j.bmcl.2008.02.080
12. Tong Y, Claiborne A, Stewart KD, Park C, Kovar P, Chen Z, Credo RB, Gu WZ, Gwaltney SL 2nd, Judge RA, Zhang H, Rosenberg SH, Sham HL, Sowin TJ, Lin NH (2007) Discovery of 1, 4-dihydroindeno[1, 2-c]pyrazoles as a novel class of potent and selective checkpoint kinase 1 inhibitors. Bioorg Med Chem 15:2759–2767. doi:10.1016/j.bmc.2007.01.012
13. Tao ZF, Wang L, Stewart KD, Chen Z, Gu W, Bui MH, Merta P, Zhang H, Kovar P, Johnson E, Park C, Judge R, Rosenberg S, Sowin T, Lin NH (2007) Structure-based design, synthesis, and biological evaluation of potent and selective macrocyclic checkpoint kinase 1 inhibitors. J Med Chem 50:1514–1527. doi:10.1021/jm061247v
14. Foloppe N, Fisher LM, Francis G, Howes R, Kierstan P, Potter A (2006) Identification of a buried pocket for potent and selective inhibition of Chk1: prediction and verification. Bioorg Med Chem 14:1792–1804. doi:10.1016/j.bmc.2005.10.022
15. Tong Y, Claiborne A, Pyzytulinska M, Tao ZF, Stewart KD, Kovar P, Chen Z, Credo RB, Guan R, Merta PJ, Zhang H, Bouska J, Everitt EA, Murry BP, Hickman D, Stratton TJ, Wu J, Rosenberg SH, Sham HL, Sowin TJ, Lin NH (2007) 1, 4-Dihydroindeno[1, 2-c]pyrazoles as potent checkpoint kinase 1 inhibitors: extended exploration on phenyl ring substitutions and preliminary ADME/PK studies. Bioorg Med Chem Lett 17:3618–3623. doi:10.1016/j.bmcl.2007.04.055

16. Ni ZJ, Barsanti P, Brammeier N, Diebes A, Poon DJ, Ng S, Pecchi S, Pfister K, Renhowe PA, Ramurthy S, Wagman AS, Bussiere DE, Le V, Zhou Y, Jansen JM, Ma S, Gesner TG (2006) 4-(Aminoalkylamino)-3-benzimidazole-quinolinones as potent CHK-1 inhibitors. Bioorg Med Chem Lett 16:3121–3124. doi:10.1016/j.bmcl.2006.03.059
17. Zhao B, Bower MJ, McDevitt PJ, Zhao H, Davis ST, Johanson KO, Green SM, Concha NO, Zhou BB (2002) Structural basis for Chk1 inhibition by UCN-01. J Biol Chem 277:46609–46615. doi:10.1074/jbc.M201233200
18. Brnardic EJ, Garbaccio RM, Fraley ME, Tasber ES, Steen JT, Arrington KL, Dudkin VY, Hartman GD, Stirdivant SM, Drakas BA, Rickert K, Walsh ES, Hamilton K, Buser CA, Hardwick J, Tao W, Beck SC, Mao X, Lobell RB, Sepp-Lorenzino L, Yan Y, Ikuta M, Munshi SK, Kuo LC, Kreatsoulas C (2007) Optimization of a pyrazoloquinolinone class of Chk1 kinase inhibitors. Bioorg Med Chem Lett 17:5989–5994. doi:10.1016/j.bmcl.2007.07.051
19. Janetka JW, Ashwell S (2009) Checkpoint kinase inhibitors: a review of the patent literature. Expert Opin Ther Pat 19:165–197. doi:10.1517/13543770802653622
20. Güner OF (2005) The impact of pharmacophore modeling in drug design. IDrugs 8:567–572
21. Khedkar SA, Malde AK, Coutinho EC, Srivastava S (2007) Pharmacophore modeling in drug discovery and development: an overview. Med Chem 3:187–197
22. Dror O, Shulman-Peleg A, Nussinov R, Wolfson HJ (2004) Predicting molecular interactions in silico: I. A guide to pharmacophore identification and its applications to drug design. Curr Med Chem 11:71–90
23. Chen JJ, Liu TL, Yang LJ, Li LL, Wei YQ, Yang SY (2009) Pharmacophore modeling and virtual screening studies of checkpoint kinase 1 inhibitors. Chem Pharm Bull (Tokyo) 57:704–709. doi:10.1248/cpb.57.704
24. Wolber G, Langer T (2005) LigandScout: 3-D pharmacophores derived from protein-bound ligands and their use as virtual screening filters. J Chem Inf Model 45:160–169. doi:10.1021/ci049885e
25. Zou J, Xie HZ, Yang SY, Chen JJ, Ren JX, Wei YQ (2008) Towards more accurate pharmacophore modeling: Multicomplex-based comprehensive pharmacophore map and most-frequent-feature pharmacophore model of CDK2. J Mol Graph Model 27:430–438. doi:10.1016/j.jmgm.2008.07.004
26. Kirchmair J, Markt P, Distinto S, Schuster D, Spitzer GM, Liedl KR, Langer T, Wolber G (2008) The Protein Data Bank (PDB), its related services and software tools as key components for in silico guided drug discovery. J Med Chem 51:7021–7040. doi:10.1021/jm8005977
27. Lloyd DG, Garcia-Sosa AT, Alberts IL, Todorov NP, Manceral RL (2004) The effect of tightly bound water molecules on the structural interpretation of ligand-derived pharmacophore models. J Comput-Aided Mol Des 18:89–100. doi:10.1023/B:jcam.0000030032.81753.b4
28. Accelrys Software Inc, Discovery Studio User Guide (June 2008) Accelrys Software Inc, San Diego
29. Barreca ML, De Luca L, Iraci N, Rao A, Ferro S, Maga G, Chimirri A (2007) Structure-based pharmacophore identification of new chemical scaffolds as non-nucleoside reverse transcriptase inhibitors. J Chem Inf Model 47:557–562. doi:10.1021/ci600320q
30. Accelrys Inc, Catalyst Version 4.10 Tutorials (January 2005) Accelrys Inc,San Diego
31. Krovat EM, Fruhwirth KH, Langer T (2005) Pharmacophore identification, in silico screening, and virtual library design for inhibitors of the human factor Xa. J Chem Inf Model 45:146–159. doi:10.1021/ci049778k
32. Wishart DS, Knox C, Guo AC, Cheng D, Shrivastava S, Tzur D, Gautam B, Hassanali M (2008) DrugBank: a knowledgebase for drugs, drug actions and drug targets. Nucleic Acids Res 36:D901–D906. doi:10.1093/nar/gkm958
33. Lin NH, Xia P, Kovar P, Park C, Chen Z, Zhang H, Rosenberg SH, Sham HL (2006) Synthesis and biological evaluation of 3-ethylidene-1, 3-dihydro-indol-2-ones as novel checkpoint 1 inhibitors. Bioorg Med Chem Lett 16:421–426. doi:10.1016/j.bmcl.2005.09.064
34. Chen Z, Xiao Z, Gu WZ, Xue J, Bui MH, Kovar P, Li G, Wang G, Tao ZF, Tong Y, Lin NH, Sham HL, Wang JY, Sowin TJ, Rosenberg SH, Zhang H (2006) Selective Chk1 inhibitors differentially sensitize p53-deficient cancer cells to cancer therapeutics. Int J Cancer 119:2784–2794. doi:10.1002/ijc.22198
35. Tao ZF, Chen Z, Bui MH, Kovar P, Johnson E, Bouska J, Zhang H, Rosenberg S, Sowin T, Lin NH (2007) Macrocyclic ureas as potent and selective Chk1 inhibitors: an improved synthesis, kinome profiling, structure-activity relationships, and preliminary pharmacokinetics. Bioorg Med Chem Lett 17:6593–6601. doi:10.1016/j.bmcl.2007.09.063
36. Kirchmair J, Ristic S, Eder K, Markt P, Wolber G, Laggner C, Langer T (2007) Fast and efficient in silico 3D screening: toward maximum computational efficiency of pharmacophore-based and shape-based approaches. J Chem Inf Model 47:2182–2196. doi:10.1021/ci700024q
37. Steindl T, Laggner C, Langer T (2005) Human rhinovirus 3C protease: generation of pharmacophore models for peptidic and nonpeptidic inhibitors and their application in virtual screening. J Chem Inf Model 45:716–724. doi:10.1021/ci049638a
38. Kirchmair J, Laggner C, Wolber G, Langer T (2005) Comparative analysis of protein-bound ligand conformations with respect to catalyst′s conformational space subsampling algorithms. J Chem Inf Model 45:422–430. doi:10.1021/ci049753l
39. Zabludoff SD, Deng C, Grondine MR, Sheehy AM, Ashwell S, Caleb BL, Green S, Haye HR, Horn CL, Janetka JW, Liu D, Mouchet E, Ready S, Rosenthal JL, Queva C, Schwartz GK, Taylor KJ, Tse AN, Walker GE, White AM (2008) AZD7762, a novel checkpoint kinase inhibitor, drives checkpoint abrogation and potentiates DNA-targeted therapies. Mol Cancer Ther 7:2955–2966. doi:10.1158/1535-7163.MCT-08-0492
40. Hahn M (1997) Three-Dimensional shape-based searching of conformationally flexible compounds. J Chem Inf Comput Sci 37:80–86. doi:10.1021/ci960108r
41. Ananthula RS, Ravikumar M, Pramod AB, Madala KK, Mahmood SK (2008) Strategies for generating less toxic P-selectin inhibitors: pharmacophore modeling, virtual screening and counter pharmacophore screening to remove toxic hits. J Mol Graph Model 27:546–557. doi:10.1016/j.jmgm.2008.09.007
42. Triballeau N, Acher F, Brabet I, Pin JP, Bertrand HO (2005) Virtual screening workflow development guided by the "receiver operating characteristic" curve approach. Application to high-throughput docking on metabotropic glutamate receptor subtype 4. J Med Chem 48:2534–2547. doi:10.1021/jm049092j
43. Pipeline Pilot, version 6.1.6.0 (2008) Scitegic, San Diego, CA